


Article

Evaluation of *Streptococcus mutans* Adhesion to Stainless Steel Surfaces Modified Using Different Topographies Following a Biomimetic Approach

Santiago Arango-Santander ^{1,*} , Lina Serna ¹, Juliana Sanchez-Garzon ^{1,2} and John Franco ^{1,3}

¹ GIOM Group, Faculty of Dentistry, Universidad Cooperativa de Colombia, Envigado 055422, Colombia; lina.sernaga@campusucc.edu.co (L.S.); juliana.sanchezga@campusucc.edu.co (J.S.-G.); john.francoa@campusucc.edu.co (J.F.)

² Faculty of Dentistry, CES University, Medellín 050021, Colombia

³ Salud y Sostenibilidad Group, School of Microbiology, Universidad de Antioquia, Medellín 050010, Colombia

* Correspondence: santiago.arango@campusucc.edu.co; Tel.: +57-4-4446065

Abstract: Bacterial adhesion to surfaces is the first step in biofilm formation, which leads to the development of conditions that may compromise the health status of patients. Surface modification has been proposed to reduce bacterial adhesion to biomaterials. The objective of this work was to assess and compare *Streptococcus mutans* adhesion to the surface of biomimetically-modified stainless steel using different topographies. Stainless steel plates were modified using a soft lithography technique following a biomimetic approach. The leaves from *Colocasia esculenta*, *Crocasmia aurea* and *Salvinia molesta* were used as surface models. Silica sol was synthesized using the sol-gel method. Following a soft lithography technique, the surface of the leaves were transferred to the surface of the SS plates. Natural and modified surfaces were characterized by means of atomic force microscopy and contact angle. *Streptococcus mutans* was used to assess bacterial adhesion. Contact angle measurements showed that natural leaves are highly hydrophobic, but such hydrophobicity could not be transferred to the metallic plates. Roughness varied among the leaves and increased after transference for *C. esculenta* and decreased for *C. aurea*. In general, two of the surface models used in this investigation showed positive results for reduction of bacterial adhesion (*C. aurea* and *C. esculenta*), while the other showed an increase in bacterial adhesion (*S. molesta*). Therefore, since a biomimetic approach using natural surfaces showed opposite results, careful selection of the surface model needs to be taken into consideration.

Keywords: surface topography; bacterial adhesion; biomimetics; soft lithography; surface modification



Citation: Arango-Santander, S.; Serna, L.; Sanchez-Garzon, J.; Franco, J. Evaluation of *Streptococcus mutans* Adhesion to Stainless Steel Surfaces Modified Using Different Topographies Following a Biomimetic Approach. *Coatings* **2021**, *11*, 829. <https://doi.org/10.3390/coatings11070829>

Academic Editor: Jun-Beom Park

Received: 8 June 2021

Accepted: 4 July 2021

Published: 9 July 2021

Publisher's Note: MDPI stays neutral with regard to jurisdictional claims in published maps and institutional affiliations.



Copyright: © 2021 by the authors. Licensee MDPI, Basel, Switzerland. This article is an open access article distributed under the terms and conditions of the Creative Commons Attribution (CC BY) license (<https://creativecommons.org/licenses/by/4.0/>).

1. Introduction

Stainless steel (SS) is a biomaterial that is highly used to manufacture devices that will be in close contact with human tissues for extended periods of time [1–3]. In the field of dentistry, particularly in orthodontics, SS is immensely used to fabricate appliances and devices, such as archwires and brackets, due to its outstanding anticorrosive properties [4–6]. However, since such devices are located within the oral cavity, they are highly susceptible to bacterial adhesion and biofilm formation due to the surface properties of this biomaterial [7–10].

Surface roughness and hydrophobicity are two of the most relevant properties involved in the process of bacterial adhesion and biofilm formation. Surface roughness promotes bacterial adhesion [11] and surface hydrophobicity allows bacterial species to adhere, colonize and grow on a surface [11,12]. Bacterial adhesion to such devices is favored by the fact that SS may have a rough surface; this adhesion will eventually lead to the formation of a mature biofilm that has the potential to cause harmful conditions to surrounding natural tissues, such as dental caries or gingivitis [13,14].

Different approaches, especially oral hygiene-related procedures, have been investigated over the years to reduce bacterial adhesion to natural and artificial surfaces [15–17]. Nonetheless, these methods have proven insufficient. An additional approach, known as surface modification, has been reported in the scientific literature in recent years. Surface modification is a vast field that includes many different chemical [18,19] and physical techniques. Topographic modifications at micro and nanometric scales is one of such physical approaches [20].

Physical surface modification techniques are divided into two large areas: top-down techniques, in which nano or microstructures are created from larger structures, and bottom-up techniques, in which larger structures are created from smaller elements [21,22]. Soft lithography belongs to the former and is a set of techniques based on self-assembly and replica molding to create micro and nano structures on the surface of materials [22,23]. Soft lithography is based upon copying and transferring the topography of a master model, which has been traditionally created using photolithography [23], to another surface. However, nature has shown, over thousands of years, that an enormous number of master models are readily available to be used for human strategies. Such inspiration in natural models is known as biomimetics [24,25]. Modified surfaces inspired by animal sources have been previously investigated [24,26], but botanical products have been scarcely used as models to modify the surface of biomaterials. Natural vegetal products, such as the leaves from Taro (*Colocasia esculenta*), Montbretia (*Crocasmia aurea*) and Giant salvinia (*Salvinia molesta*) display particular surface features, including water repellency and self-cleaning abilities, that may be interesting when considering using natural surfaces as models for surface modification [23].

Surface modification to reduce bacterial adhesion has been studied and reported in the scientific literature over the last years. Different authors have demonstrated that bacterial adhesion is reduced to physically modified surfaces [27,28]. Biomimetics has served as inspiration to other authors to emulate natural patterns, like the shark skin, and transfer them to the surface of biomaterials [29], while other investigations have shown that the topography of natural leaves reduces bacterial adhesion on SS and titanium alloy orthodontic wires [30]. However, even though the reported results are highly promising, information on using botanical sources as models to modify the surface of biomaterials is scarce and only a few plants or leaves have been reported.

Therefore, the objective of this work was to modify the surface of SS plates using the topography from three natural leaves and compare the adhesion of *Streptococcus mutans* to such modified surfaces.

2. Materials and Methods

2.1. Substrates

Stainless steel 316L (SS316L) plates (Onlinemetals.com, Seattle, WA, USA) with dimensions of 1.0 cm × 1.0 cm × 1.0 mm were used. Plates were sequentially polished using silicon carbide abrasive papers (400–1200 grit, Abracol, Colombia) and a mirror-like surface was obtained using diamond paste (0.5 µm, Leco Corporation, St. Joseph, MI, USA). SS plates were then sequentially cleaned in an ultrasonic bath using 99.8% acetone (Merck Millipore, Burlington, MA, USA), distilled water (Protokimica, Medellin, Colombia) and 99% ethanol (Merck Millipore, Burlington, MA, USA). Plates were allowed to dry in air and were divided into four groups, one of them regarded as the control group (polished SS 316L).

2.2. Master Model

The lamina of the leaves from Taro (*Colocasia esculenta*), Montbretia (*Crocasmia aurea*) and Giant salvinia (*Salvinia molesta*) were used to fabricate the master models. Such leaves were selected because they show high hydrophobicity and self-cleaning properties at simple observation without technical equipment.

2.3. Sol-Gel Synthesis

Silica sol was synthesized following the one-stage sol-gel method [31]. Tetraethylorthosilicate (TEOS) and methyltriethoxysilane (MTES) (ABC R GmbH & Co., Karlsruhe, Germany) were used as silica precursors, 0.1 N nitric acid (Merck Millipore, Burlington, MA, USA) and acetic acid (glacial, 100% *v/v*, Merck Millipore, Burlington, MA, USA) were used as catalyzers and absolute ethanol (99.9% *v/v*, Merck Millipore, Burlington, MA, USA) was used as solvent. Final silica concentration was 18 g·L⁻¹. The sol was synthesized in a thermostatic bath at 40 °C under constant stirring at 300 rpm for 3 h. It was stored at 4 °C for 24 h before using.

2.4. Soft Lithography

For the three experimental groups, the corresponding natural leaves were cut in 5.0 cm-diameter segments. These fragments were located at the bottom of silicone containers with the lamina of the leaf facing upward. Polydimethylsiloxane (PDMS, Silastic T-2, Dow Corning Corporation, Midland, MI, USA) was used to duplicate the topography of each leaf. To obtain the stamp, PDMS was prepared according to the manufacturer and was poured to cover each fragment. Polymerization for 24 h was allowed, followed by further heat treatment at 80 °C for 3 h to finish the process. PDMS stamps containing the topography from each leaf were obtained. To transfer the topography from each stamp to the corresponding SS 316L plate, a drop of 7 µL of silica sol was placed on the SS surface, the stamp was placed on top of the drop and gentle pressure was applied to distribute the sol throughout the surface. Gelation was allowed for 4 h at RT and then the stamp was removed. The plates from the experimental groups were subjected to heat treatment at 450 °C for 30 min. After this procedure, three experimental groups were obtained (one group per topography).

2.5. Surface Characterization

The natural leaves, polished SS 316L plates and transferred plates from the three experimental groups were characterized by means of atomic force microscopy (AFM, Nanosurf Easyscan 2, Nanosurf AG, Liestal, Switzerland), to determine the surface roughness, and contact angle (CA) method to assess surface hydrophobicity. For AFM acquisition, a NCLR tip (Nanosensors™, Neuchâtel, Switzerland) in tapping mode at a constant force of 48 N/m was used. AFM images were processed using AxioVision software (V 4.9.1.0, Carl Zeiss Microscopy GmbH, Jena, Germany), Image J software (1.51 J, Laboratory for Optical and Computational Instrumentation, University of Wisconsin, Madison, WI, USA) [32] and WSxM software (5.0, Nanotec Electronic and New Microscopy Laboratory, Madrid, Spain) [33]. 10 AFM images of 50 × 50 µm² per group were used to obtain the arithmetic average of the roughness profile (Ra) using the Gwyddion software (2.34, Department of Nanometrology, Czech Metrology Institute, Brno, Czech Republic). For surface hydrophobicity, the sessile drop method was used on 10 plates from each group. A camera (Canon EOS Rebel XS, Tokyo, Japan) and a macro lens (105 mm F2.8 EX DG OS, Sigma, Ronkonkoma, NY, USA) were used to obtain the images and the angle values were obtained using software AxioVision (V. 4.9.1.0).

2.6. Bacterial Adhesion Test

Streptococcus mutans (ATCC 25175, Microbiologics, St. Cloud, MN, USA) was used to assess bacterial adhesion to control and experimental surfaces following a previously validated protocol [30,34]. *S. mutans* was grown in Brain Heart Infusion (BHI) agar (Scharlab S.L., Barcelona, Spain) supplemented with 0.2 U/mL bacitracin (Sigma Fluka, St. Louis, MO, USA) followed by incubation for 24 h at 37 ± 1 °C. Then, *S. mutans* was cultured in peptone water for 24 h at 37 ± 1 °C. The bacterial suspension was centrifuged at 5000 × *g* for 15 min, supernatant was discarded and the bacterial pellet was re-suspended in peptone water at 10⁷ CFU/mL by measuring the nephelometric turbidity unit (NTU) (based on a calibration curve of NTU vs. CFU/mL). 15 plates from control and each experimental

group were used for bacterial adhesion tests. Each plate from each group was placed at the bottom of the well of a 24-well non-treated polystyrene plate (Costar, Corning Inc., NY, USA) and 500 μL of the bacterial solution was added to cover each SS 316L plate. Polystyrene plates were incubated for 8 h at 37 ± 1 $^{\circ}\text{C}$ to allow bacterial adhesion. After this time, experimental and control plates were carefully rinsed three times with 0.9% saline solution (Corpaul, Medellin, Colombia) to remove non-adherent bacterial cells. Then, each sample was subjected to sonication (Qsonica 125, Newtown, CT, USA) at 50% power for 3 sec to quantify viable adherent bacteria. Sonicated solutions were serially diluted and 10 μL were cultured in BHI agar, by triplicate, following the drop plate method [35]. Culture plates were incubated for 48 h at 37 ± 1 $^{\circ}\text{C}$ and then Colony Forming Units (CFU) were counted.

2.7. Statistical Analyses

Comparative analysis of roughness for the natural leaves was performed by the Student's *t*-test for independent variables (results from *S. molesta* were excluded). Hydrophobicity results were compared using the Kruskal-Wallis H test and post-hoc analysis with the Mann Whitney U test and Bonferroni correction. Comparison of hydrophobicity and bacterial adhesion among transferred plates was performed by the one-factor Anova test and multiple comparisons through the Tukey's HSD test. Roughness results among transferred plates were compared using the Kruskal-Wallis H test and post-hoc analysis with the Mann Whitney U test and Bonferroni correction. Bivariate analysis tests were performed after previous verification of compliance with the assumptions of normality and homoscedasticity of the variances through the statistics of Shapiro Wilk and Levene, respectively. Values of $p < 0.05$ were considered statistically significant. Software SPSS (V. 25) was used for statistical analyses.

3. Results

3.1. Surface Characterization of Natural Leaves

Figure 1 shows AFM images of the polished SS 316L control plate and *C. esculenta* and *C. aurea* natural leaves. AFM images of *S. molesta* could not be obtained due to the topographical features on the surface of the leaf, which prevented the tip from making close contact with the surface.

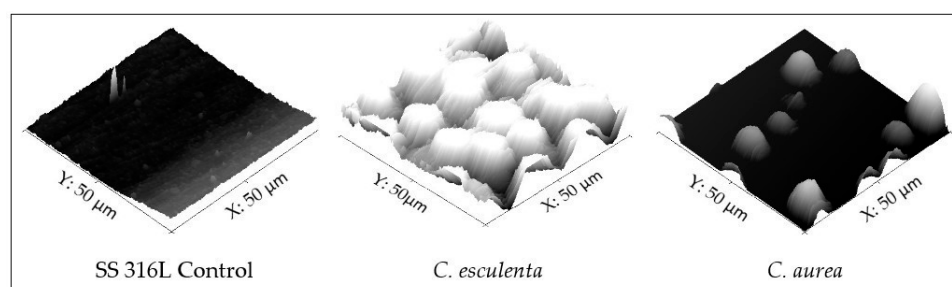


Figure 1. AFM images of a polished SS 316L (control) plate, *C. esculenta* and *C. aurea* leaves.

Contact angle measurements from the three natural leaves exhibited high hydrophobicity (contact angle $> 120^{\circ}$). The most hydrophobic leaf was *S. molesta*, followed by *C. aurea* and *C. esculenta* (Figure 2). The differences were statistically significant ($p < 0.001$).

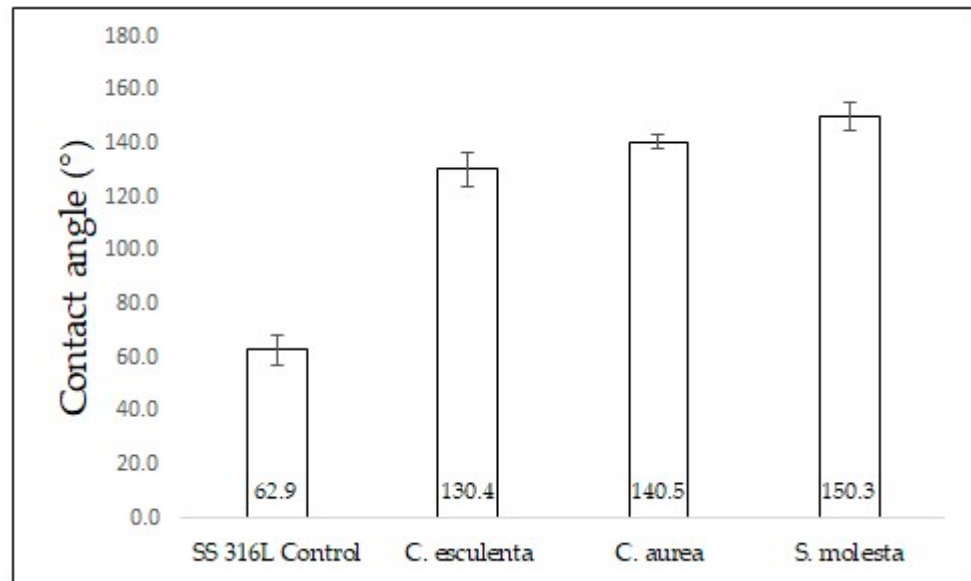


Figure 2. Contact angle measurements of control (SS 316L) surface and natural leaves.

As for roughness of the natural leaves, *C. aurea* showed higher roughness than *C. esculenta* and the difference was statistically significant ($p < 0.001$, Figure 3). As already mentioned, roughness of *S. molesta* could not be determined by AFM.

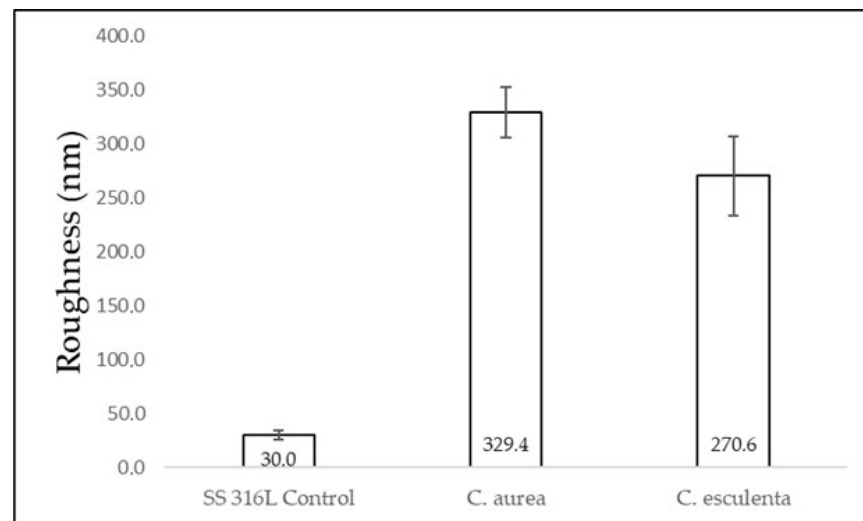


Figure 3. Average roughness of control (SS 316L) surface and natural leaves.

3.2. Surface Characterization of Modified and Control Surfaces

Regarding surface hydrophobicity of the transferred surfaces, CA measurements from plates modified with the different topographies showed higher values than the control surface. The highest CA was found for the experimental surface modified using the *C. esculenta* leaf model, followed by *S. molesta* y *C. aurea*, respectively. The difference between control and modified surfaces was statistically significant ($p < 0.001$). In addition, the difference in CA between the experimental surface modified with the *C. esculenta* leaf (highest CA value) and *C. aurea* (lowest CA value) was statistically significant ($p = 0.004$, Figure 4).

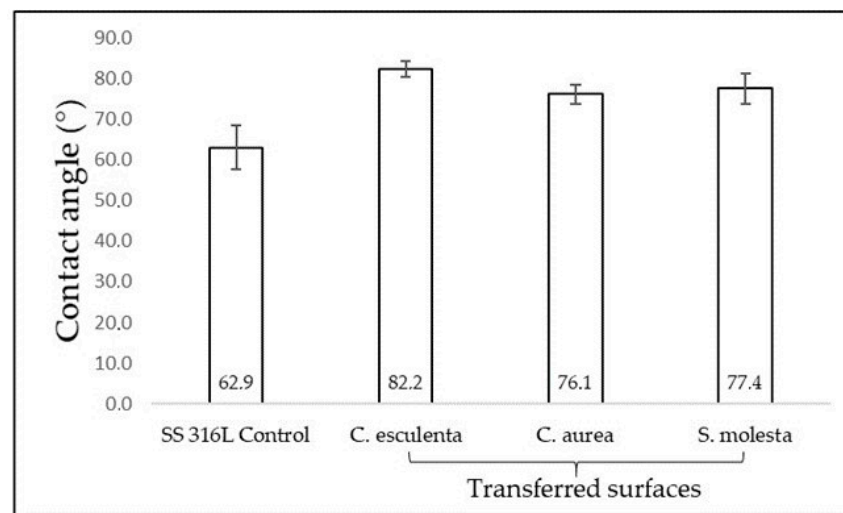


Figure 4. Contact angle measurements from control (SS 316L) and transferred (experimental) surfaces.

When comparing surface roughness from modified surfaces versus SS 316L control, the former showed higher R_a values, and the plates modified using the *C. aurea* leaf showed the highest values, followed by *C. esculenta* and SS 316L control. The difference between modified surfaces and SS 316L control was statistically significant ($p < 0.001$, Figure 5). In addition, the R_a values from the plates modified using the *C. aurea* leaf were lower than the respective natural leaf. In contrast, the R_a values from the plates modified using the *C. esculenta* leaf were higher than the respective natural leaf (data not shown). Such comparison could not be made for *S. molesta* since R_a values could not be obtained for the natural leaf as explained above.

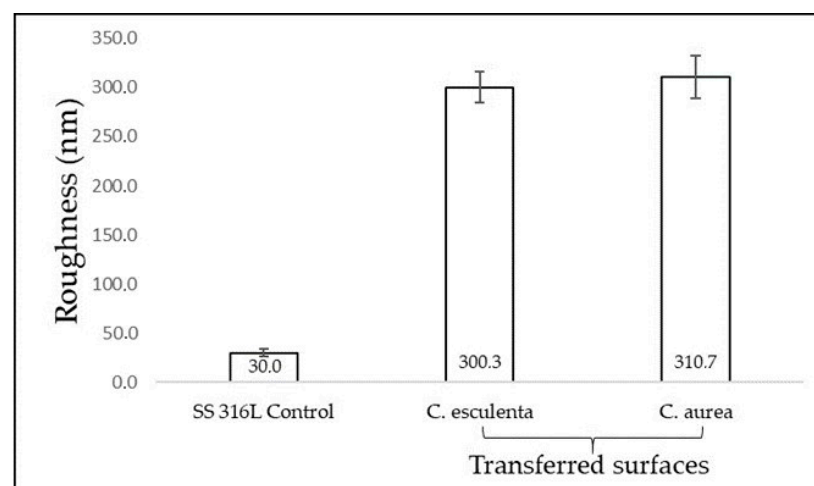


Figure 5. Average roughness of control (SS316L) and transferred (experimental) surfaces.

3.3. Evaluation of *S. mutans* Adhesion

The values from the plates modified using the *C. aurea* leaf showed the lowest adhesion ($1.3 \times 10^6 \pm 2.5 \times 10^5$ CFU/surface) when compared to control surface ($1.9 \times 10^6 \pm 2.5 \times 10^5$ CFU/surface) and the other two experimental surfaces ($1.9 \times 10^6 \pm 2.4 \times 10^5$ CFU/surface and $2.3 \times 10^6 \pm 5.0 \times 10^5$ CFU/surface for *C. esculenta* and *S. molesta*, respectively). The difference was statistically significant ($p < 0.001$). The modified surface using the *C. esculenta* leaf showed lower adhesion than the plate modified with the *S. molesta* topography. However, the values from *C. esculenta* modification and SS 316L were similar and the difference was not statistically significant (Figure 6). In addition, when comparing

the *S. mutans* adhesion to the plates modified using the *S. molesta* topography versus the other treatments, including the control surface, higher values were found

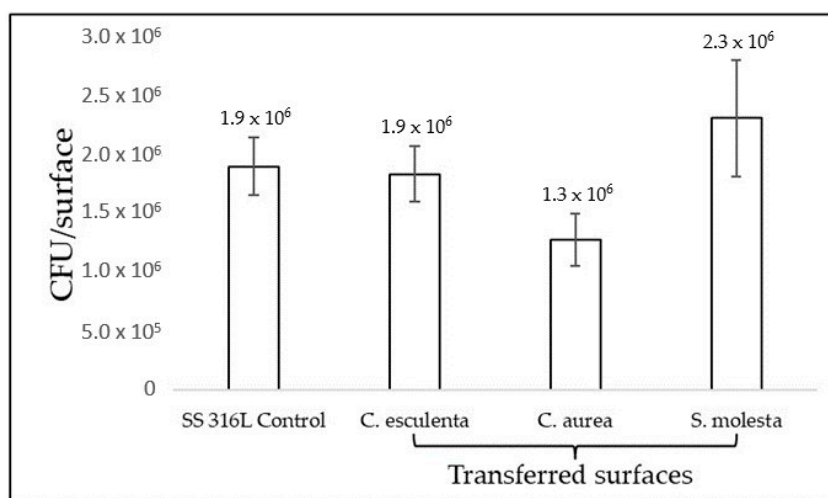


Figure 6. *S. mutans* adhesion to control (SS 316L) and transferred (experimental) surfaces.

4. Discussion

In recent years, different papers have addressed the subject of how topographic modifications on the surface of biomaterials may assist in reducing bacterial adhesion and biofilm formation [27–29]. The current investigation assessed *S. mutans* adhesion to the surface of surgical-grade stainless steel plates that were modified using different topographies following biomimetic inspiration. Natural patterns were selected based on their ability to self-clean and the apparent high hydrophobicity exhibited in their natural environment (water-repellency).

The topography of the natural leaves used as models was assessed and relevant properties were measured. They showed high hydrophobicity (130.4° for *C. esculenta*, 140.5° for *C. aurea* and 150.3° for *S. molesta*, on average). According to hydrophobicity values presented by Kim and Choi [36] and Falde et al. [37], only the *S. molesta* leaf could be classified as superhydrophobic (CA $> 150^\circ$), while *C. esculenta* and *C. aurea* were classified as hydrophobic (CA between 90° and 150°). Jaggessar et al. [38] reported a contact angle between 90° and 150° for *C. esculenta*, which is in agreement with the values obtained in the present work. For comparison purposes, no values could be found for *C. aurea* and *S. molesta* in the scientific literature.

Then, a comparison between the hydrophobicity values from the natural surfaces and the values from the transferred surfaces was performed and a reduction in the contact angle measurement after the transference was found in all cases. Even though there was a reduction in hydrophobicity values, they were still higher than SS 316L. This finding may have different explanations. Biological surfaces, including natural leaves, may have protective coatings made of natural waxes that increase the hydrophobicity and such coatings could not be transferred to stainless steel plates using soft lithography [36–41]. In addition, silica sol-gel was used to transfer the topography from each leaf to polished SS 316L. Several authors [42–44] have found that when silica sol synthesized with similar TEOS:MTES ratios as the ones in the current investigation is used to coat SS surfaces, an increase in hydrophobicity is found due to the presence of methyl groups from the silica that reduce the ability of the surface to absorb water [44]. Therefore, the presence of silica may explain why the hydrophobicity values from the transferred surfaces are higher than the value from polished SS 316L. However, this effect of silica on stainless steel is not as strong as the effect that a protective wax coating has in the natural plants and leaves, hence, the values from natural sources are significantly higher than those from the transferred surfaces, which are, in turn, higher than silica-free SS 316L.

Regarding roughness, the values from the *S. molesta* leaf could not be obtained using AFM due to the topography of this natural surface consisting of multiple macrometric hair-like structures that prevented the tip from making close contact with the surface, which is necessary to obtain a correct reading. The topography of a given sample is one of the limitations exhibited by AFM, especially when the sample has steeply inclined surfaces [45], such as the topographic features shown by *S. molesta*, even at higher scales. The roughness of the remaining natural leaves (*C. aurea* and *C. esculenta*) was similar, but when comparing the roughness from the natural leaves and the transferred surfaces, an increase in roughness was observed for *C. esculenta* and a reduction was found for *C. aurea*. Such reduction in roughness may be explained by the fact that biological surfaces could have a hierarchical structure and intricate architecture [40,46] and the transfer process employed in this protocol used smooth silica sol, which may have filled some of the irregularities on the surface, hence the reduction that was observed. An explanation for the increase in roughness in the transfer of *C. esculenta* remains to be elucidated.

As for bacterial adhesion, surface roughness and hydrophobicity play a major role in how bacterial species adhere to a surface and form a biofilm. De la Pinta et al. [47] found that more abundant biofilm was formed on rougher surfaces, but such results could not be correlated when hydrophobicity was considered. Raspor et al. [48] assessed bacterial adhesion to five SS 304 surfaces to determine the influence of roughness on adhesion. They found that adhesion increases as roughness increases. Bohinc et al. [49] also obtained similar results on glass. Díaz et al. [50,51] demonstrated that roughness at the nano scale reduces bacterial adhesion, while roughness at the micro scale increases it. Xu et al. [52] confirmed such findings and explained that such reduction at the nano scale is due to the narrow space available for the bacterium and the obstacle that this represents for bacterial aggregation, which had been previously established by Hochbaum and Aizenberg [27]. These findings are conflicting with the results of the current work, since the rougher topography (*C. aurea*) showed the lower bacterial adhesion. This may be explained by the fact that, even though both the modified surface using the *C. aurea* model and the actual leaf showed higher roughness values, its apparently more organized topography and/or the size of its surface features related to the size of the bacterial species used [27] were responsible for the reduction in bacterial adhesion.

When analyzing the relation between hydrophobicity and bacterial adhesion, the higher the CA value, the lower the *S. mutans* adhesion. The most hydrophobic surface (*S. molesta*) showed an increase in bacterial adhesion, while the less hydrophobic surfaces (*C. aurea* and *C. esculenta*) exhibited lower adhesion of this bacterial species. Since it was not possible to obtain the roughness value from *S. molesta*, it is not possible to determine that the increase in bacterial adhesion is solely ascribable to its hydrophobicity, but a combination of high hydrophobicity and an apparent high roughness. It is important to notice that the difference in the relation between hydrophobicity and bacterial adhesion between the current investigation and the work by De la Pinta et al. [47] may be due to the bacterial species under evaluation, since more hydrophobic species prefer more hydrophobic surfaces. In the current work, *S. mutans* showed lower adhesion to more hydrophobic surfaces, which is in agreement with the results by Satou et al. [53], who demonstrated that *S. mutans* is a hydrophilic bacterial species that show more affinity to hydrophilic surfaces.

Adhesion to topographically modified surfaces has been addressed in the literature for a few years. Vladillo-Rodriguez et al. [54] created engineered nano surfaces and assessed bacterial adhesion. They concluded that different surface patterns caused reduction of bacterial adhesion ranging from 40% to over 95%. Bhardwaj and Webster [55] modified titanium substrates and found a 95% reduction in *Staphylococcus aureus* adhesion, a 90% reduction in *Pseudomonas aeruginosa* adhesion and a 81% reduction in *Escherichia coli* adhesion.

When modifications were based on natural models (biomimetics), Carman et al. [56] used a surface based on the sharkskin, known as Sharklet, and found a reduction in the aggregation of spores from green algae. May et al. [28], Chung et al. [29] and Reddy et al. [57]

found a reduction in bacterial adhesion to modified surfaces, using patterns from the Sharklet model, on different materials. Bixler et al. [24] evaluated anti-fouling properties of microstructures based on butterfly wings and rice leaves and obtained promising results. However, most works on surface modification using bio-inspired or biomimetic approaches are based on surfaces obtained from animal models, while plants offer many possibilities that need to be evaluated. Previous works using surface modification based on a natural leaf (*C. esculenta*) have also demonstrated a reduction in bacterial adhesion to SS and titanium surfaces [30,34]. Since *C. aurea* showed better results than *C. esculenta* for reduction in bacterial adhesion in the current work, future investigations using botanical materials as models to modify biomaterials surfaces must be continued.

5. Conclusions

Within the limitations of the current investigation, a topographic modification of the smooth surface of a metallic biomaterial showed reduction in bacterial adhesion. Three different topographies from natural leaves (*C. aurea*, *C. esculenta* and *S. molesta*) were used, but only surfaces based on *C. aurea* and *C. esculenta* models showed such effect, even though there was an increase in roughness after every transference. There were also a reduction in the hydrophobicity after the transference due to hierarchical features and protective coatings that soft lithography is incapable of transferring. The most hydrophobic surfaces showed higher bacterial adhesion, which is also related to the bacterial species used in the current investigation. The results in bacterial adhesion suggests a relation between roughness, hydrophobicity and topographic features that is relevant to reduce the adhesion of this bacterial species to the surface of SS. Such reduction is important in short term investigations because it opens new possibilities in the field of using materials and surfaces that nature has to offer to improve biomaterials for medical and dental applications. However, due to conflicting results obtained in the present work, careful attention must be given to the selection of the natural surface.

Author Contributions: Conceptualization, S.A.-S.; Data curation, J.S.-G. and J.F.; Formal analysis, J.S.-G. and J.F.; Investigation, S.A.-S. and L.S.; Methodology, S.A.-S. and L.S.; Project administration, S.A.-S.; Supervision, S.A.-S. and J.S.-G.; Writing—original draft, S.A.-S. and L.S.; Writing—review & editing, S.A.-S., J.S.-G. and J.F. All authors have read and agreed to the published version of the manuscript.

Funding: This research received no external funding.

Institutional Review Board Statement: Not applicable.

Informed Consent Statement: Not applicable.

Data Availability Statement: The data presented in this study are available on request from the corresponding author.

Acknowledgments: The authors would like to thank Claudia García from Universidad Nacional de Colombia for her assistance with the sol-gel method and Johanna Gutiérrez from Tecnoacademia for her assistance with the AFM.

Conflicts of Interest: The authors declare no conflict of interest.

References

1. Robert, M.; Ezzell, J. *Regulatory Affairs for Biomaterials and Medical Devices*, 1st ed.; McGraw Hill: New York, NY, USA, 2014.
2. Patel, N.R.; Gohil, P.P. A review on biomaterials: Scope, applications & human anatomy significance. *IJETAE* **2012**, *2*, 91–101.
3. Watts, D. Orthodontic adhesive resins. In *Orthodontic Material: Scientific and Clinical Aspects*, 1st ed.; Thieme Medical Publ Inc.: Stuttgart, Germany, 2001; pp. 202–217.
4. Oh, K.T.; Choo, S.U.; Kim, K.M.; Kim, K.N. A stainless steel bracket for orthodontic application. *Eur. J. Orthod.* **2005**, *27*, 237–244. [[CrossRef](#)]
5. Pérez, L.; Garmas, E. Mini implantes, una opción para el anclaje en ortodoncia. *Gac. Médica Espirituana* **2010**, *12*, 1–9. Available online: <http://revgmespirituana.sld.cu> (accessed on 10 March 2021).

6. Uribe, G.; Aristiz, J.F. Metales y Alambres De Ortodoncia. In *Ortodoncia Teoría y Clínica*, 1st ed.; Marcolud: Bogota, Colombia, 2004; pp. 226–245.
7. Ábalos, C. Adhesión bacteriana a biomateriales. *Av. Odontostomatol.* **2005**, *21*, 347–353. [[CrossRef](#)]
8. Koch, K.; Barthlott, W. Superhydrophobic and superhydrophilic plant surfaces: An inspiration for biomimetic materials. *Philos. Trans. R. Soc. A Math. Phys. Eng. Sci.* **2009**, *367*, 1487–1509. [[CrossRef](#)]
9. Berg, J.M.; Romoser, A.; Banerjee, N.; Zebda, R.; Sayes, C.M. The relationship between pH and zeta potential of ~30 nm metal oxide nanoparticle suspensions relevant to in vitro toxicological evaluations. *Nanotoxicology* **2009**, *3*, 276–283. [[CrossRef](#)]
10. Kiremitçi-Gümü, M. Microbial adhesion to ionogenic PHEMA, PU and PP implants. *Biomaterials* **1996**, *17*, 443–449. [[CrossRef](#)]
11. Abrams, G.A.; Teixeira, A.I.; Nealey, P.F.; Murphy, C.J. Effects of substratum topography on cell behavior. *Biomim. Mater. Des.* **2002**, *33*, 91–137.
12. Zhang, X.; Wang, L.; Levänen, E. Superhydrophobic surfaces for the reduction of bacterial adhesion. *RSC Adv.* **2013**, *3*, 12003–12020. [[CrossRef](#)]
13. Pitts, N.B.; Zero, D.T.; Marsh, P.D.; Ekstrand, K.; Weintraub, J.A.; Ramos-Gomez, F.; Tagami, J.; Twetman, S.; Tsakos, G.; Ismail, A. Dental caries. *Nat. Rev. Dis. Primers* **2017**, *3*, 1–16. [[CrossRef](#)]
14. Moulis, E.; Chabadel, O.; Goldsmith, M.C.; Canal, P. Prevención de caries y ortodoncia. *EMC-Pediatría* **2008**, *43*, 1–9. [[CrossRef](#)]
15. Marsh, P.D. Are dental diseases examples of ecological catastrophes? *Microbiology* **2003**, *149*, 279–294. [[CrossRef](#)]
16. Teles, R.P.; Teles, F.R.F. Antimicrobial agents used in the control of periodontal biofilms: Effective adjuncts to mechanical plaque control? *Braz. Oral Res.* **2009**, *23*, 39–48. [[CrossRef](#)] [[PubMed](#)]
17. Bradshaw, D.J. To the control of oral biofilms. *Adv. Dent. Res.* **1997**, *11*, 176–185.
18. Hall-Stoodley, L.; Nistico, L.; Sambanthamoorthy, K.; Dice, B.; Nguyen, D.; Mershon, W.J.; Johnson, C.; Hu, F.Z.; Stoodley, P.; Ehrlich, G.D.; et al. Characterization of biofilm matrix, degradation by DNase treatment and evidence of capsule downregulation in *Streptococcus pneumoniae* clinical isolates. *BMC Microbiol.* **2008**, *8*, 1–16. [[CrossRef](#)] [[PubMed](#)]
19. Darouiche, R.O.; Mansouri, M.D.; Gawande, P.V.; Madhyastha, S. Antimicrobial and antibiofilm efficacy of triclosan and DispersinB[®] combination. *J. Antimicrob. Chemother.* **2009**, *64*, 88–93. [[CrossRef](#)]
20. Biswas, A.; Bayer, I.S.; Biris, A.S.; Wang, T.; Dervishi, E.; Faupel, F. Advances in top-down and bottom-up surface nanofabrication: Techniques, applications & future prospects. *Adv. Colloid Interface Sci.* **2012**, *170*, 2–27.
21. Arango, S.; Peláez-Vargas, A.; García, C. Coating and surface treatments on orthodontic metallic materials. *Coatings* **2012**, *3*, 1–15. [[CrossRef](#)]
22. Xia, Y.; Whitesides, G. Soft lithography. *Annu. Rev. Mater. Sci.* **1998**, *28*, 153–184. [[CrossRef](#)]
23. Whitesides, G.M.; Ostuni, E.; Jiang, X.; Ingber, D.E. Soft lithography in biology. *Annu. Rev. Biomed. Eng.* **2001**, *3*, 335–373. [[CrossRef](#)]
24. Bixler, G.D.; Theiss, A.; Bhushan, B.; Lee, S.C. Anti-fouling properties of microstructured surfaces bio-inspired by rice leaves and butterfly wings. *J. Colloid Interface Sci.* **2014**, *419*, 114–133. [[CrossRef](#)]
25. Rocha-Rangel, E. Biomimética: De la naturaleza a la creación humana. *Ciencias* **2010**, *4*, 1–8.
26. Bhadra, C.M.; Khanh Truong, V.; Pham, V.T.H.; Al Kobaisi, M.; Seniutinas, G.; Wang, J.Y.; Juodkazis, S.; Crawford, R.J.; Ivanova, E.P. Antibacterial titanium nano-patterned arrays inspired by dragonfly wings. *Sci. Rep.* **2015**, *5*, 16817. [[CrossRef](#)]
27. Hochbaum, A.; Aizenberg, J. Bacteria pattern spontaneously on periodic nanostructure arrays. *Nano Lett.* **2010**, *10*, 3717–3721. [[CrossRef](#)]
28. May, R.M.; Hoffman, M.G.; Sogo, M.J.; Parker, A.E.; O’Toole, G.A.; Brennan, A.B.; Reddy, S.T. Micro-patterned surfaces reduce bacterial colonization and biofilm formation in vitro: Potential for enhancing endotracheal tube designs. *Clin. Transl. Med.* **2014**, *3*, 1–8. [[CrossRef](#)]
29. Chung, K.K.; Schumacher, J.F.; Sampson, E.M.; Burne, R.A.; Antonelli, P.J.; Brennan, A.B. Impact of engineered surface microtopography on biofilm formation of *Staphylococcus aureus*. *Biointerphases* **2007**, *2*, 89–94. [[CrossRef](#)]
30. Arango-Santander, S.; Gonzalez, C.; Aguilar, A.; Cano, A.; Castro, S.; Sanchez-Garzon, J.; Franco, J. Assessment of streptococcus mutans adhesion to the surface of biomimetically-modified orthodontic archwires. *Coatings* **2020**, *10*, 201. [[CrossRef](#)]
31. Arango-Santander, S.; Freitas, S.; Pelaez-Vargas, A.; Garcia, C. Silica sol-gel patterned surfaces based on dip-pen nanolithography and microstamping: A comparison in resolution and throughput. *Key Eng. Mater.* **2016**, *720*, 264–268. [[CrossRef](#)]
32. Schneider, C.A.; Rasband, W.S.; Eliceiri, K.W. NIH image to ImageJ: 25 years of image analysis. *Nat. Methods* **2012**, *9*, 671–675. [[CrossRef](#)] [[PubMed](#)]
33. Horcas, I.; Fernández, R.; Gómez-Rodríguez, J.M.; Colchero, J.; Gómez-Herrero, J.; Baro, A.M. WSXM: A software for scanning probe microscopy and a tool for nanotechnology. *Rev. Sci. Instrum.* **2007**, *78*, 1–8. [[CrossRef](#)] [[PubMed](#)]
34. Arango-Santander, S.; Pelaez-Vargas, A.; Freitas, S.; García, C. Surface modification by combination of dip-pen nanolithography and soft lithography for reduction of bacterial adhesion. *J. Nanotech.* **2018**, *2018*, 1–10. [[CrossRef](#)]
35. Naghili, H.; Tajik, H.; Mardani, K.; Razavi Rouhani, S.M.; Ehsani, A.; Zare, P. Validation of drop plate technique for bacterial enumeration by parametric and nonparametric tests. *Vet. Res. Forum* **2013**, *4*, 179–183.
36. Kim, J.; Choi, S.O. Superhydrophobicity. Waterproof and water repellent textiles and clothing. In *The Textile Institute Book Series*; Woodhead Publishing: Sawston, UK, 2018; pp. 267–297.
37. Falde, E.; Yohe, S.; Colson, Y.; Grinstaff, M. Superhydrophobic materials for biomedical applications. *Biomaterials* **2016**, *104*, 87–103. [[CrossRef](#)]

38. Jaggesar, A.; Shahali, H.; Mathew, A.; Yarlagadda, P. Bio-mimicking nano and micro-structured surface fabrication for antibacterial properties in medical implants. *J. Nanobiotech.* **2017**, *15*, 1–20. [[CrossRef](#)]
39. Burton, Z.; Bhushan, B. Surface characterization and adhesion and friction properties of hydrophobic leaf surfaces. *Ultramicroscopy* **2006**, *106*, 709–719. [[CrossRef](#)] [[PubMed](#)]
40. Grewal, H.; Cho, I.; Yoon, E. The role of bio-inspired hierarchical structures in wetting. *Bioinspiration Biomim.* **2015**, *10*, 026009. [[CrossRef](#)] [[PubMed](#)]
41. Bhushan, B. Biomimetics: Lessons from nature—An overview. *Philos. Trans. R. Soc. A* **2009**, *367*, 1445–1486. [[CrossRef](#)] [[PubMed](#)]
42. Santos, O.; Nylander, T.; Rosmaninho, R.; Rizzo, G.; Yiantsios, S.; Andritsos, N.; Karabelas, A.; Müller-Steinhagen, H.; Melo, L.; Boulangé-Petermann, L.; et al. Modified stainless steel surfaces targeted to reduce fouling—Surface characterization. *J. Food Eng.* **2004**, *64*, 63–79. [[CrossRef](#)]
43. Hosseinalipour, S.M.; Ershad-langroudi, A.; Hayati, A.N.; Nabizade-Haghighi, A.M. Characterization of sol-gel coated 316L stainless steel for biomedical applications. *Prog. Org. Coat.* **2010**, *67*, 371–374. [[CrossRef](#)]
44. Yang, H.; Pi, P.; Cai, Z.Q.; Wen, X.; Wang, X.; Cheng, J.; Yang, Z. Facile preparation of super-hydrophobic and super-oleophilic silica film on stainless steel mesh via sol-gel process. *Appl. Surf. Sci.* **2010**, *256*, 4095–4102. [[CrossRef](#)]
45. Haßler-Grohne, W.; Hüser, D.; Klaus-Peter, J.; Frase, C.; Bosse, H. Current limitations of SEM and AFM metrology for the characterization of 3D nanostructures. *Meas. Sci. Technol.* **2011**, *22*, 1–8. [[CrossRef](#)]
46. Xiang, Y.; Huang, S.; Huang, T.; Dong, A.; Cao, D.; Li, H.; Xue, Y.; Lv, P.; Duan, H. Superrepellency of underwater hierarchical structures on salvinia leaf. *Proc. Natl. Acad. Sci. USA* **2020**, *117*, 2282–2287. [[CrossRef](#)] [[PubMed](#)]
47. De-la-Pinta, I.; Cobos, M.; Ibarretxe, J.; Montoya, E.; Eraso, E.; Guraya, T.; Quindós, G. Effect of biomaterials hydrophobicity and roughness on biofilm development. *J. Mater. Sci. Mater. Med.* **2019**, *30*, 77. [[CrossRef](#)]
48. Raspor, P.; Bohinc, K.; Dražić, G.; Fink, R.; Oder, M.; Jevšnik, M.; Nipič, D. Available surface dictates microbial adhesion capacity. *Inter. J. Adhes. Adhes.* **2014**, *50*, 265–272.
49. Bohinc, K.; Dražić, G.; Abram, A.; Jevšnik, M.; Jeršek, B.; Nipič, D.; Kurinčič, M.; Raspor, P. Metal surface characteristics dictate bacterial adhesion capacity. *Inter. J. Adhes. Adhes.* **2016**, *68*, 39–46. [[CrossRef](#)]
50. Díaz, C.; Schilardi, P.; Salvarezza, R.; Fernández Lorenzo de Mele, M. Nano/microscale order affects the early stages of biofilm formation on metal surfaces. *Langmuir* **2007**, *23*, 11206–11210. [[CrossRef](#)] [[PubMed](#)]
51. Diaz, C.; Schilardi, P.; dos Santos Claro, P.C.; Salvarezza, R.C.; Fernandez Lorenzo de Mele, M. Submicron trenches reduce the *Pseudomonas fluorescens* colonization rate on solid surfaces. *Appl. Mater. Interfaces* **2009**, *1*, 136–143. [[CrossRef](#)]
52. Xu, L.C.; Siedlecki, C.A. Submicron-textured biomaterial surface reduces staphylococcal bacterial adhesion and biofilm formation. *Acta Biomater.* **2012**, *8*, 72–81. [[CrossRef](#)]
53. Satou, J.; Fukunaga, A.; Satou, N.; Shintani, H.; Okuda, K. Streptococcal adherence on various restorative materials. *J. Dent. Res.* **1988**, *67*, 588–591. [[CrossRef](#)]
54. Vadillo-Rodríguez, V.; Guerra-García-Mora, A.; Perera-Costa, D.; González-Martín, M.; Fernández-Calderón, M. Bacterial response to spatially organized microtopographic surface patterns with nanometer scale roughness. *Colloids Surf. B Biointerfaces* **2018**, *169*, 340–347. [[CrossRef](#)]
55. Bhardwaj, G.; Webster, T.J. Reduced bacterial growth and increased osteoblast proliferation on titanium with a nanophase TiO₂ surface treatment. *Inter. J. Nanomed.* **2017**, *12*, 363–369. [[CrossRef](#)] [[PubMed](#)]
56. Carman, M.; Estes, T.; Feinberg, A.; Schumacher, J.; Wilkerson, W.; Wilson, L.; Callow, M.; Callow, J.; Brennan, A. Engineered antifouling microtopographies—Correlating wettability with cell attachment. *Biofouling* **2006**, *22*, 11–21. [[CrossRef](#)] [[PubMed](#)]
57. Reddy, S.; Chung, K.; McDaniel, C.; Darouiche, R.; Landman, J.; Brennan, A. Micropatterned surfaces for reducing the risk of catheter-associated urinary tract infection: An in vitro study on the effect of sharklet micropatterned surfaces to inhibit bacterial colonization and migration of uropathogenic *Escherichia coli*. *J. Endourol.* **2011**, *25*, 1547–1552. [[CrossRef](#)] [[PubMed](#)]